COO-3058-44

LINEAR ACCELERATOR PROJECT

AEC Contract No. AT(11-1)-3058

PROGRESS REPORT

for

October 1, 1973 - December 31, 1973

Rensselaer Polytechnic Institute
Troy, New York 12181

Erwin R. Gaerttner
Project Director

DISCLAIMER

TABLE OF CONTENTS

NEUTRON CROSS SECTIONS

KEV NEUTRON CAPTURE CROSS SECTION OF ^{105}Pd, ^{151}Eu AND ^{153}Eu

H. D. Knox,* R. W. Hockenbury, N. N. Kaushal and R. C. Block+

Preliminary results of neutron capture measurements on the separated isotopes of ^{105}Pd, ^{151}Eu and ^{153}Eu are presented. The experiment was performed using the Rensselaer LINAC and the 1.25-meter capture detection at 25 meters. The relative neutron flux was measured using a ^{10}B-NaI detector and ENDF/III boron cross sections for its relative efficiency calculation.

Results are presented in Table 1. The capture data are normalized using published resonance parameters.[1,2] (This normalization will be confirmed later when our own capture and total cross-section data in the resolved resonance region have been analyzed.) Sample thicknesses were chosen to minimize self-shielding corrections in the keV region and are generally less than 2%.

The statistical precision of the capture cross sections is approximately ±4%. The uncertainty in normalization is ±12%, mostly due to the uncertainty in the resonance parameters upon which the normalization is based.

The ^{151}Eu and ^{153}Eu results are about 10-18% higher than the smooth curves shown in Ref. 1. The ^{151}Eu capture cross section result is in excellent agreement in the 8-12 keV range of overlap with that of Czirr.[3]

---

*Now at Texas A&M University, College Station, Texas.
+On Sabbatical at Kyoto University, Japan.

Table 1. KeV Capture Cross Sections[1]

ENERGY[2] (keV)	^{105}Pd (bns)	^{151}Eu (bns)	^{153}Eu (bns)
4	2.83[3]	14.3[4]	10.2[4]
8	2.98	11.0	6.96
12	2.84	8.60	5.75
16	2.08	6.74	4.90
20	2.03	5.79	4.28
24	1.63	5.04	3.75
28	1.66	4.49	3.49
65	1.06	2.56	2.30

1. Statistical Uncertainty ±4%
   Normalization Uncertainty ±12%
2. The results shown represent local averages over a few data points around the energies indicated.
3. Normalized to resonance parameters in BNL-325, Supp. 2, 2nd Ed.
4. Normalized to resonance parameters in Col. report (F. J. Rahn), NYO-72-281, UC-34 (Physics).

REFERENCES:

1. BNL-325, Supp. 2, 2nd Ed.
2. F. J. Rahn, NYO-72-281, UC-34.
3. J. B. Czirr, "^{165}Ho, ^{151}Eu and Natural Eu Capture Cross-Section Measurements," UC-34, TID-4500.

4354

NUBAR RATIOS AT THERMAL ENERGIES FOR ^{233}U, ^{235}U AND ^{239}Pu

R. W. Hockenbury

The ratios of prompt nubar ($\bar{\nu}$) at 0.025 eV are of interest in the evaluation of all the measured parameters (σ_γ, σ_f, η, α, etc.) for ^{233}U, ^{235}U and ^{239}Pu.

The nubar experiments at Rensselaer measured the relative value ($\epsilon\bar{\nu}$) where ϵ is the detector efficiency. A small ^{252}Cf fission chamber was used simultaneously for normalization and monitoring purposes. By using the ratio of $(\epsilon\bar{\nu})233/(\epsilon\bar{\nu})252$ to that for ^{239}Pu, $(\epsilon\bar{\nu})239/(\epsilon\bar{\nu})252$, a comparison can be made to the ratio $\bar{\nu}(233)/\bar{\nu}(239)$ derived from absolute $\bar{\nu}$ measurements.

The actual comparison was made to prompt nubar values from a least squares fitting program[1] used in connection with the Cross Section Evaluation Working Group Subcommittee on Normalization and Standards.

The most meaningful comparison is that of the ratio of $\bar{\nu}(233)/\bar{\nu}(239)$ since our relative experiments on these two isotopes were performed under the same conditions. The results, in Table 1, show excellent agreement with the ratio of the least squares values.[1]

A comparison was also made between thermal ratios of $\bar{\nu}(233)/\bar{\nu}(235)$ and $\bar{\nu}(239)/\bar{\nu}(235)$ to our relative ratios. In both cases, our relative ratios are about 1% higher; however, since our ^{235}U relative nubar measurements were performed under different conditions of detector efficiency; this difference is not unexpected.

Table 1. Ratio of Prompt Thermal Nubar

RPI $\dfrac{(\epsilon\bar{\nu})233/(\epsilon\bar{\nu})252}{(\epsilon\bar{\nu})239/(\epsilon\bar{\nu})252}$	Ref. 1 - $\dfrac{\bar{\nu}(233)}{\bar{\nu}(239)}$
0.8622 ± 0.0051	0.8636 ± 0.0053

REFERENCE:

1. J. R. Stehn, private communication.

NEUTRON CAPTURE CROSS SECTION OF ^{242}Pu IN THE KEV ENERGY REGION

A. J. Sanislo,* N. N. Kaushal and R. W. Hockenbury

Data were taken using the 1.25-meter liquid scintillation detector system and the PDP-7. The high-low bias procedure was used to separate fission and capture events. Sodium, aluminum, cobalt and sulfur resonance filters were used to determine the time-dependent background.

The experiments covered a neutron energy range from 0.1 to 80 keV, thus providing data in the resolved resonance region as well as the keV range. Transmission data were taken over about the same energy span for normalization purposes.

The sample weight is 7.765 grams with purity as follows:

Pu^{238}	-	.022%
Pu^{239}	-	1.49 %
Pu^{240}	-	2.90 %
Pu^{241}	-	3.04 %
Pu^{242}	-	92.55 %
Pu^{244}	-	.002%

The experimental statistics in the keV range vary from 8-10% on a channel-by-channel basis including the uncertainty due to the background correction. Excellent data were also obtained in the resolved resonance region with some peaks over 20,000 counts per channel. A few impurity resonances have been identified; deadtime and background corrections are being made.

*Based in part on the Master of Science Thesis of A. J. Sanislo.

CAPTURE AND TOTAL CROSS-SECTION MEASUREMENTS ON ^{54,58}Fe AND ^{61,64}Ni

M. Pandey,* N. N. Kaushal, R. Garg,# H. D. Knox,† R. C. Block+ and R. W. Hockenbury

Analysis of the low and high resolution capture data is continuing on all four isotopes. High resolution transmission experiments are being set up for ^{54}Fe, ^{58}Fe and ^{61}Ni. (The low resolution transmission data already obtained on ^{64}Ni are adequate for the available sample.) The plans for the high resolution transmission experiment include a linac pulse width of 11 ns, channel width of 8 ns and a flight path of 28 m. The energy range of interest is about 14 to 200 keV.

*Based in part on the Ph.D. Thesis of M. Pandey, State University of New York at Albany.

#State University of New York at Albany.

†Now at Texas A&M University, College Station, Texas.

+On Sabbatical at Kyoto University, Japan.

REACTOR PHYSICS AND ENGINEERING - EXPERIMENTAL

ASSESSMENTS OF CROSS-SECTION DATA FILES FOR SODIUM

A. N. Mallen,* N. N. Kaushal, B. K. Malaviya
and E. R. Gaerttner

Following is the summary of a paper submitted for presentation at the 1974 Annual Meeting of the American Nuclear Society, to be held in Philadelphia, Pennsylvania in June, 1974.

ABSTRACT

Extensive time-of-flight measurements of position- and angle-dependent neutron spectra in a large homogeneous assembly have been performed and analyzed to check the basic cross-section data sets for sodium.[1]

The experimental arrangement has been described previously.[2] The measured spectra were compared with one-dimensional S_N transport calculations[3] using cross sections from the ENDF/B-I and ENDF/B-III data files. The cross sections were processed through the SUPERTOG[4] code to obtain 49-group P_8 scattering matrices for the transport calculations.

Figure 1 shows the high energy neutron spectra (E > 10 keV) for the source and the forward-directed zero-degree flux ($\mu = 1.0$) for radial positions $R_A = 10.5$ inches and $R_B = 18.5$ inches. The spectra have been normalized to the source. The comparison transport calculations are based on a 49-group ENDF/B-III[5] cross section set using P_8 scattering (employing the consistent transport quadrature), and the black absorber model[6] for the source representation. The agreement between the measurements and calculations is excellent, in terms of both attenuation and spectral shape.

Figure 2 shows the angular spectra for radius R = 34.5 inches. The calculations employed the ENDF/B-I data set and are a composite of two 49 energy-group fluxes joined to form a single 66-group spectrum between 100 eV and 10 MeV. The experimental data were normalized to the theory at 380 keV. The overall spectral shape agreement is very good. The apparent discrepancy at the 2.85

---

*Based in part on the Ph.D. Thesis of A. N. Mallen.
Present address: Savannah River Laboratory, Aiken, South Carolina.

keV resonance is due to a 4% resolution broadening of the experimental data because of uncertainty in mean emission times.[7] Above 4 MeV, discrepancies increase with increasing angle (decreasing μ). Three possible reasons for the discrepancy are (a) a known 30% peak in the high energy (E > 3.0 MeV) neutron emission from the target along the centerline of the assembly (μ = 0) which was not accounted for in the calculations, and (b) the increase in high energy flux (magnitude unknown) due to the reentrant hole perturbation[8] which increases with increasing angle (decreasing μ) or (c) the possible need for an angular redistribution of the high energy elastic scattering differential cross section. Effects (a) and (b) together can be entirely responsible for the high energy discrepancy and (c) may be unjustified.

The ENDF/B-I and ENDF/B-III data files are very similar in predicting spectra and differ by no more than 20%. ENDF/B-III provides a better representation of the high energy flux E > 4 MeV because it predicts a flux that is ~20% higher than ENDF/B-I. For E < 10 keV, ENDF/B-III predicts a 10% to 20% lower flux than ENDF/B-I and provides a better representation for energies below 3 keV, and above 6 keV, but a poorer representation between 3 and 6 keV. Between 10 keV and 560 keV, both data sets produce similar results. Between 560 keV and 1.2 MeV, an area of great importance in fast reactors, ENDF/B-I provides a better representation because inelastic scattering in this range is about 10% lower than ENDF/B-III.

REFERENCES:

1. A. N. Mallen, Ph.D. Thesis, RPI, Troy, New York, August 1973.
2. A. N. Mallen, N. N. Kaushal, B. K. Malaviya, E. R. Gaerttner, "Measurement and Analysis of Fast Neutron Spectra in Sodium," Trans. Am. Nucl. Soc. 16, 304 (1973).
3. K. D. Lathrop, "DTF-IV - A Fortran IV Program for Solving the Multigroup Transport Equation with Anisotropic Scattering," LA 3373 (1965).
4. R. Q. Wright, N. M. Greene, J. L. Lucius, C. W. Craven, Jr., "SUPERTOG: A Program to Generate Fine Group Constants and P_n Scattering Matrices from ENDF/B," ORNL-TM-2679, Oak Ridge National Laboratory (1969).
5. T. A. Pitterle and N. C. Paik, "Studies of Applications of Cross-Section Data and Critical Experiment to Reactor Design," WARD-3045 T4B-2, Westinghouse Electric Corporation (1972).
6. B. K. Malaviya, N. N. Kaushal, M. Becker, E. T. Burns, A. Ginsberg and E. R. Gaerttner, "Experimental and Analytical Studies of Fast Neutron Transport in Iron," Nucl. Sci. Eng. 47, 329 (1972).
7. N. N. Kaushal, B. K. Malaviya, A. N. Mallen and E. R. Gaerttner, "Neutron Emission-Time Effects in a Pulsed Sodium Assembly," Trans. Am. Nucl. Soc. 15, 899 (1972).
8. M. Danchak, "Reentrant Hole Effects in Three-Dimensional Pulsed Neutron Assemblies," Master's Thesis, RPI, Troy, New York (1973).

FIGURE CAPTIONS

Fig. 1 Comparison of Zero-degree High-energy Neutron Spectra -- Measured and Calculated (Source Normalized).

Fig. 2 Comparison of Low-energy Measured and Calculated Spectra for R = 34.5 Inches (Amplitude Normalized).

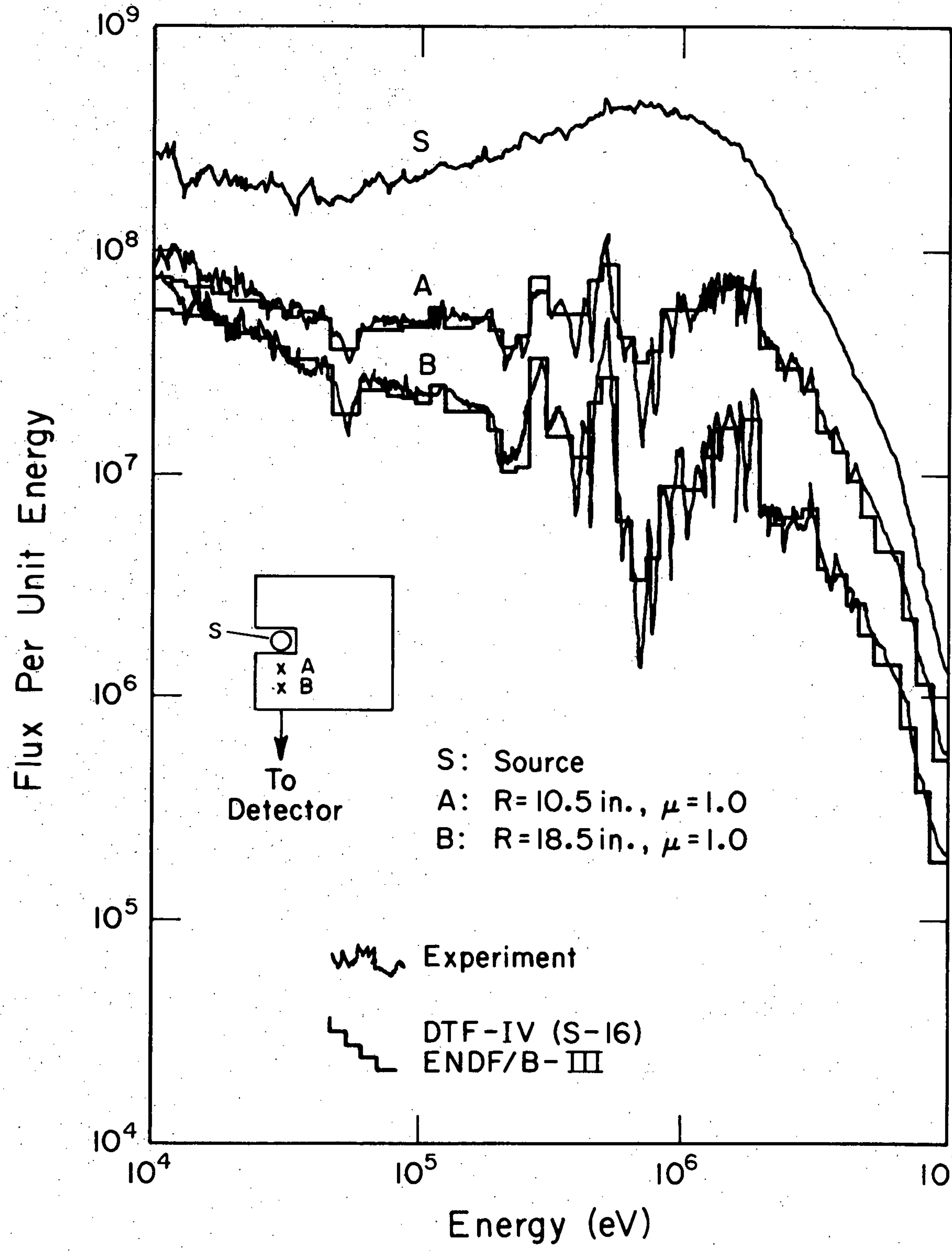

Flux Per Unit Energy
Energy (eV)
S
A
B
S
x A
x B
To Detector
S: Source
A: R=10.5 in., μ=1.0
B: R=18.5 in., μ=1.0
Experiment
DTF-IV (S-16)
ENDF/B-III

Figure 1

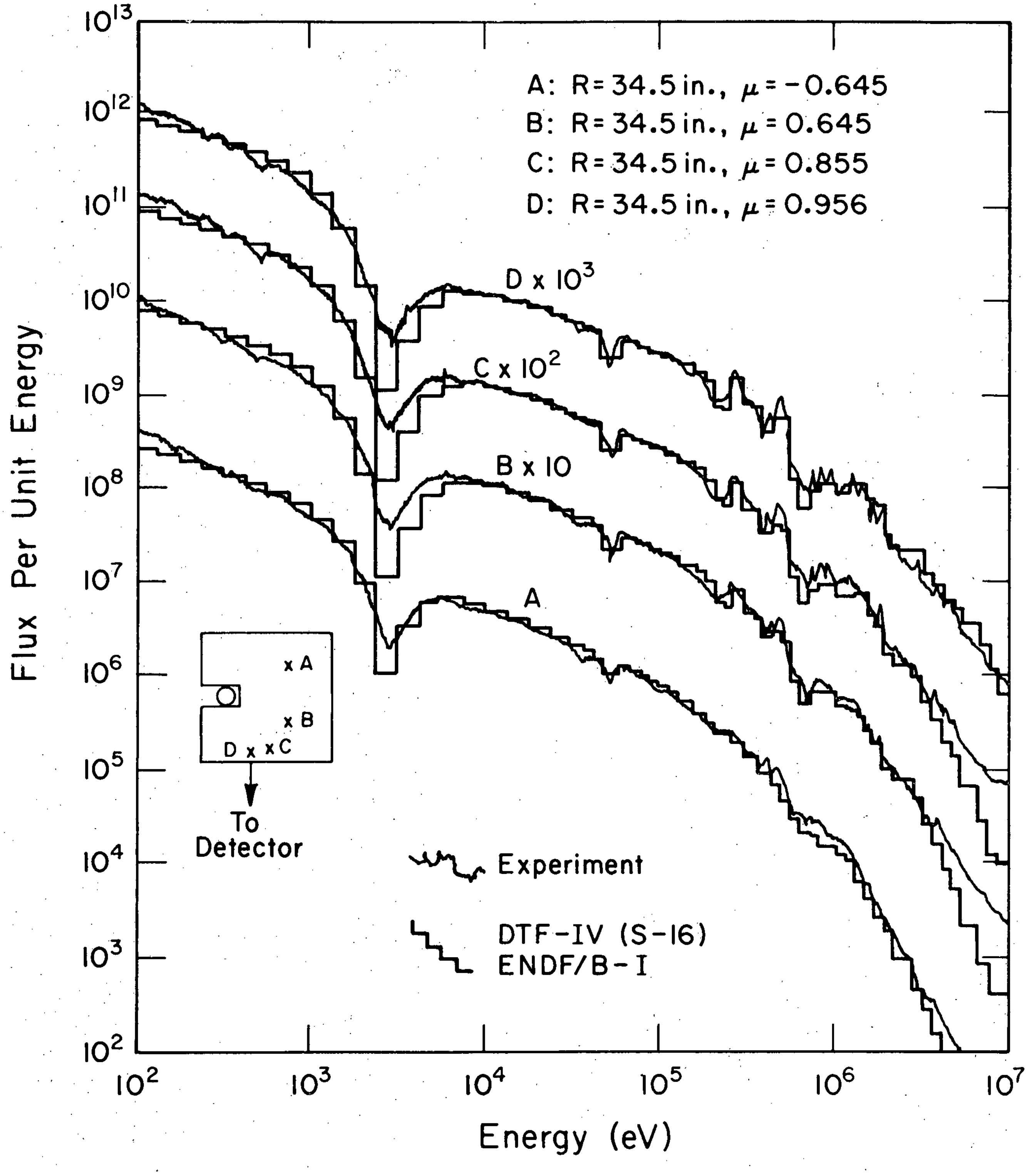
A: R = 34.5 in., μ = −0.645
B: R = 34.5 in., μ = 0.645
C: R = 34.5 in., μ = 0.855
D: R = 34.5 in., μ = 0.956
D x 10^3
C x 10^2
B x 10
A
x A
x B
D x x C
To Detector
Experiment
DTF-IV (S-16)
ENDF/B-I
Flux Per Unit Energy
Energy (eV)

Figure 2

REACTOR PHYSICS AND ENGINEERING - THEORETICAL

REACTOR THEORY AND ANALYSIS

M. Becker

Fast spectra in iron have been analyzed using data files of the ENDF/B-3 generation. The particular files are MAT 1124, the original ENDF/B-3 iron file, and MAT 4180, a file similar to the final ENDF/B-3 iron file, modified somewhat at Oak Ridge National Laboratory. Data was processed at Oak Ridge by R. Q. Wright using SUPERTOG and incorporating the RPI modifications. The SUPERTOG output was converted to transport code input at RPI using a slightly modified version of the Oak Ridge DLC-II code so as to create P8 input using the consistent Pn approximation.

Comparison of calculation with experiment so far has yielded very substantial discrepancies. However, past experience with MAT 1124 data using a scalar flux weighting spectrum characteristic of ENDF/B-1 (MAT 1020) yielded reasonably good agreement with experiment.

To check the sensitivity of the multigroup data to the weighting spectrum, additional calculations were performed, with the cooperation of Oak Ridge, for scalar spectra of the form

$$\phi_s(E) = \frac{1}{E(N\sigma_t + \frac{B^2}{3N\sigma_t})} \qquad (1)$$

for bucklings of .003 and .005 cm^{-2}. Group scattering cross sections are given in Table 1 along with those for zero buckling (the reference case) and for the ENDF/B-1 weighting spectrum. It may be observed that substantial reductions in various groups occur.

At high energies (above about 3 MeV), all cross sections are quite similar. At about 3 MeV, group scattering cross sections using Eq. (1) weighting begin to get noticeably smaller than those obtained with an ENDF/B-1 based weighting spectrum. By 1 MeV the disparity has reached about fifteen percent, and some substantially larger disparities are observed as energy decreases. Below

100 keV, with some isolated exceptions, group constants are again in agreement. It should be recalled that flux tends to go as the inverse three-halves power of age and age tends to go inversely with the square of the cross section. Thus, these cross-section discrepancies tend to be amplified in their effects on spectral shape. The expectation is that lower cross sections will yield stronger spectral attenuation. The experiment-theory discrepancy is of this character, namely excessively strong spectral attenuation relative to measurement. Again, the ENDF/B-1 weighting spectrum group set yielded good general agreement with experiment.

To understand the relation between group constants and weighting spectra under conditions of fluctuating cross sections, consider an extreme case in which the cross section is

$$\sigma = \begin{array}{ll} \sigma_0 & u_{g-1}<u<u_{g-1}+v \\ \sigma_1 & u_{g-1}+v<u<u_g \end{array} \tag{2}$$

Using Eq. (1) converted to lethargy for weighting, we may define

$$\sigma_g = \frac{\int_{u_{g-1}}^{u_g} \sigma(u)\ \emptyset_s(u)du}{\int_{u_{g-1}}^{u_g} \emptyset_s(u)du} \tag{3}$$

which becomes, using Eq. (2)

$$\sigma_g = \frac{\dfrac{\sigma_0}{N\sigma_0 + \dfrac{B^2}{3N\sigma_0}}(v-u_{g-1}) + \dfrac{\sigma_1}{N\sigma_1 + \dfrac{B^2}{3N\sigma_1}}(u_g-v)}{\left(\dfrac{1}{N\sigma_0 + \dfrac{B^2}{3N\sigma_0}}\right)(v-u_{g-1}) + \left(\dfrac{1}{N\sigma_1 + \dfrac{B^2}{3N\sigma_1}}\right)(u_g-v)} \tag{4}$$

Let us now consider some special cases with Eq. (4). Consider first the case of the buckling being rigorously zero. Equation (4) becomes

$$\sigma_g = \frac{(u_g-u_{g-1})}{\frac{v-u_{g-1}}{\sigma_0} + \frac{u_g-v}{\sigma_1}} = \frac{\sigma_1(u_g-u_{g-1})}{\frac{\sigma_1}{\sigma_0}(v-u_{g-1}) + u_g-v} \tag{5}$$

Now consider the limit as σ_1 gets very small

$$\lim_{\sigma_1 \to 0} \sigma_g = 0 \tag{6}$$

Thus, with a zero-buckling weighting spectrum, if the cross section goes to zero for a finite interval within the group, the entire group cross section will go to zero. Excessive leakage and spectral attenuation would occur.

Next, let the buckling be finite. Then Eq. (4) would become

$$\sigma_g = \frac{(v-u_{g-1}) \dfrac{1}{1 + \dfrac{B^2}{3N^2\sigma_0{}^2}} + (u_g-v) \dfrac{\sigma_1^2}{\sigma_1^2 + \dfrac{B^2}{3N^2}}}{\dfrac{v-u_{g-1}}{\sigma_0} \dfrac{1}{1 + \dfrac{B^2}{3N^2\sigma_0{}^2}} + (u_g-v) \dfrac{\sigma_1}{\sigma_1^2 + \dfrac{B^2}{3N^2}}} \tag{7}$$

Now if we consider the limit as σ_1 gets very small

$$\lim_{\sigma_1 \to 0} \sigma_g = \sigma_0 \tag{8}$$

The second term in the numerator and the second term in the denominator each would vanish and all other factors would cancel, leaving us with Eq. (8), independent of the magnitude of the buckling.

Obviously, this bar-graph type of cross section behavior does not occur. However, deep dips do. The prospect of the group cross section vanishing completely if the actual cross section vanishes anywhere, as in Eq. (6), and the prospect of the group cross section being insensitive to the vanishing of the actual cross section anywhere within the group are both unattractive. The trend of Eq. (6) may explain the low group constants in Table 1.

It thus appears that when substantial cross-section fluctuations occur, conventional general arguments for assigning weighting spectra can become questionable. Further attention shall be devoted to the problem of weighting spectra.

Table 1. MAT 1124 Group Scattering Cross Sections with Different Weighting Spectra

Group	Top Energy (MeV)	Eq.1, B^2=0	Eq.1, B^2=.003	Eq.1, B^2=.005	ENDF/B-1
1	10	1.77	1.77	1.77	1.78
2	8.82	1.86	1.86	1.86	1.87
3	7.79	1.97	1.97	1.97	1.98
4	6.87	2.22	2.22	2.22	2.23
5	5.35	2.27	2.27	2.27	2.28
6	4.72	2.24	2.24	2.24	2.24
7	4.17	2.26	2.26	2.26	2.27
8	3.68	2.19	2.19	2.19	2.21
9	3.25	2.30	2.30	2.30	2.32
10	2.87	2.41	2.42	2.42	2.45
11	2.23	2.35	2.36	2.36	2.41
12	1.97	2.19	2.20	2.20	2.33
13	1.74	2.22	2.23	2.23	2.36
14	1.53	1.89	1.90	1.91	2.10
15	1.35	1.95	1.98	2.00	2.29
16	1.19	1.57	1.59	1.60	1.80
17	1.05	1.88	1.91	1.92	2.20
18	.821	3.23	3.24	3.25	3.59
19	.724	1.68	1.77	1.82	2.36
20	.639	1.68	1.72	1.74	2.06
21	.564	2.48	2.50	2.51	2.80
22	.498	2.72	2.81	2.84	3.30
23	.439	4.39	4.41	4.41	4.87
24	.388	1.50	1.63	1.69	2.28
25	.302	2.20	2.24	2.26	2.57
26	.266	2.56	2.57	2.58	2.69
27	.235	2.65	2.67	2.68	2.94
28	.207	2.74	3.37	3.60	5.66
29	.183	1.91	1.96	1.99	2.80
30	.161	2.36	2.48	2.54	3.60
31	.126	2.15	2.15	2.15	2.16
32	..111	3.45	3.46	3.46	3.52
33	.0980	4.72	4.73	4.72	4.79
34	.0865	3.49	3.57	3.62	7.81
35	.0764	2.55	2.60	2.62	3.73
36	.0674	3.22	3.22	3.22	3.25
37	.0595	4.97	4.97	4.97	5.00
38	.0463	5.24	5.24	5.24	5.24
39	.0409	6.61	6.67	6.61	6.62
40	.0361	10.02	10.02	10.02	9.99
41	.0318	28.02	28.02	28.02	29.20
42	.0281	3.35	3.61	3.75	4.98
43	.0248	.58	.67	.71	.48
44	.0193	1.73	1.75	1.74	1.73
45	.0170	2.32	2.32	2.32	2.32
46	.0150	2.87	2.87	2.87	2.86
47	.0133	3.45	3.45	3.46	3.46
48	.0117	4.27	4.27	4.27	4.26